JOURNAL OF VIROLOGY, Sept. 2010, p. 8926–8936 Vol. 84, No. 17
0022-538X/10/$12.00 doi:10.1128/JVI.00787-10

Molecular Basis of Neurovirulence of Flury Rabies Virus Vaccine Strains: Importance of the Polymerase and the Glycoprotein R333Q Mutation▽

Lihong Tao,[1] Jinying Ge,[1] Xijun Wang,[1] Hongyue Zhai,[1] Tao Hua,[1] Bolin Zhao,[1] Dongni Kong,[1] Chinglai Yang,[2] Hualan Chen,[1]* and Zhigao Bu[1]*

Veterinary Public Health Laboratory of Ministry of Agriculture and State Key Laboratory of Veterinary Biotechnology, Harbin Veterinary Research Institute of Chinese Academy of Agricultural Sciences, Harbin 150001, People's Republic of China,[1] and Department of Microbiology and Immunology, Emory University School of Medicine, Rollins Research Center, Atlanta, Georgia 30322[2]

Received 14 April 2010/Accepted 4 June 2010

The molecular mechanisms associated with rabies virus (RV) virulence are not fully understood. In this study, the RV Flury low-egg-passage (LEP) and high-egg-passage (HEP) strains were used as models to explore the attenuation mechanism of RV. The results of our studies confirmed that the R333Q mutation in the glycoprotein (G_{R333Q}) is crucial for the attenuation of Flury RV in mice. The R333Q mutation is stably maintained in the HEP genome background but not in the LEP genome background during replication in mouse brain tissue or cell culture. Further investigation using chimeric viruses revealed that the polymerase L gene determines the genetic stability of the G_{R333Q} mutation during replication. Moreover, a recombinant RV containing the LEP G protein with the R333Q mutation and the HEP L gene showed significant attenuation, genetic stability, enhancement of apoptosis, and immunogenicity. These results indicate that attenuation of the RV Flury strain results from the coevolution of G and L elements and provide important information for the generation of safer and more effective modified live rabies vaccine.

Rabies virus (RV) belongs to the genus *Lyssavirus* of the family *Rhabdoviridae* and causes a fatal neurological disease in humans and animals (6). The RV genome is a nonsegmented negative-strand (NNS) RNA encoding five structural proteins: nucleoprotein (N), phosphoprotein (P), matrix protein (M), glycoprotein (G), and large polymerase (L). Among these, the G protein is a major contributor to RV pathogenicity (7, 31, 33). The G protein facilitates fast virus entry and transsynaptic spread and regulates the rate of virus replication, together with other viral elements (8, 30, 39). The G protein of nonpathogenic RV strains can trigger apoptosis, while the RV G of pathogenic strains induces less or no apoptosis (35, 59). The amino acid residue at position 333 of the G protein (G333) of some fixed strains has been shown to be an important determinant of virulence in adult mice (5). Strains that have arginine or lysine at position G333 kill adult mice, whereas mutants with other amino acids at this site cause a nonlethal infection (1, 5, 25, 36, 49, 53). However, the pathogenicity of RV strains is not solely determined by substitutions at the G333 position. Other substitutions in the G protein, such as N194K, have also been shown to affect viral pathogenicity in mice (10, 21, 50). In addition, other viral elements, such as the N, P, M, and L genes, the trailer sequence in the noncoding region, and the pseudogene, were also reported to modulate RV pathogenicity (12, 46, 57, 58). How these viral elements regulate the pathogenicity of RV remains to be fully explored, and further investigation is needed to understand the molecular basis of RV pathogenicity.

Attenuated Flury RV low-egg-passage (LEP) and high-egg-passage (HEP) strains were established through serial passage in chicken brain, chicken embryos, and culture cells using a Flury RV isolated from a girl who died of rabies (23, 24). LEP has Arg at position G333 and kills adult mice after intracerebral (i.c.) inoculation, while HEP has Gln at G333 and causes only mild signs in adult mice. It has been demonstrated that HEP could regain lethality in adult mice by a single amino acid change at G333 from Gln to Arg (49), which indicated that Arg at position G333 is a key determinant of pathogenicity of Flury RV in adult mice. However, whether the Arg at G333 is indispensable for the lethal phenotype of LEP has not been demonstrated.

In the current study, LEP and HEP Flury RV strains were used as models to investigate the mechanism of attenuation. We found that both G and L contribute to the attenuation of Flury RV. Substitution of Arg with Gln at G333 (G_{R333Q}) eliminated LEP neuroinvasiveness but not the virus' lethal phenotype in adult mice after i.c. inoculation. The G_{R333Q} mutation could be kept stable only in the genome background of HEP but not in that of LEP during replication. The L gene contributes to the attenuation and enhanced immunogenicity of Flury RV by promoting the stabilization of the G_{R333Q} mutation during virus replication in brain tissues or cells.

* Corresponding author. Mailing address: Harbin Veterinary Research Institute of CAAS, 427 Maduan Street, Harbin 150001, People's Republic of China. Phone for Zhigao Bu: 86-451-85935062. Fax: 86-451-82733132. E-mail: zgbu@yahoo.com. Phone for Hualan Chen: 86-451-85935079. Fax: 86-451-82733132. E-mail: hlchen1@yahoo.com.
▽ Published ahead of print on 10 June 2010.

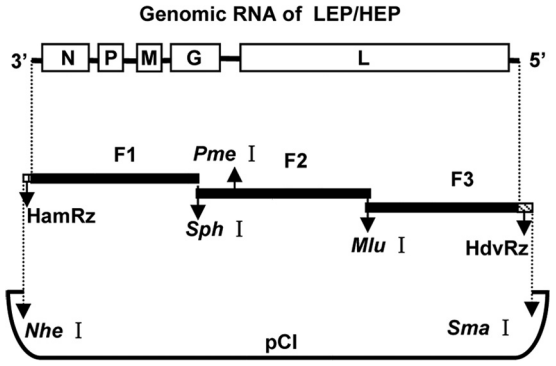

FIG. 1. Schematic representation of the construction of full-length cDNA plasmids of Flury LEP and HEP strains. The cDNA fragments F1, F2, and F3 were reverse transcribed and amplified from LEP/HEP RNA and subcloned stepwise into the pCI vector. The hammerhead ribozyme sequence (HamRz) was introduced upstream of the LEP/HEP genome in fragment F1, and the hepatitis delta virus ribozyme sequence (HdvRz) was introduced downstream of the viral genome.

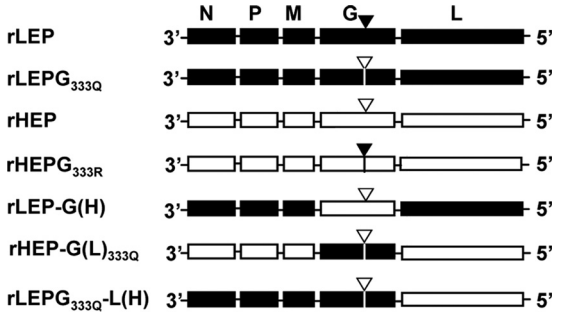

FIG. 2. Genomic structures of rescued RVs rLEP and rHEP and their mutants and chimeras. The black and white bars represent the genes that originate from the LEP and HEP strains, respectively. Solid and open inverted triangles indicate the amino acid at G333 (▼, Arg; ▽, Gln).

MATERIALS AND METHODS

Viruses and cells. Neuroblastoma (NA) cells of A/J mouse origin were grown in Eagle's minimum essential medium (MEM) supplemented with 10% fetal bovine serum (FBS). Baby hamster kidney (BHK-21) cells were grown in Dulbecco's modified Eagle's MEM (DMEM) supplemented with 10% FBS. The RV Flury strains LEP (AV2012) and HEP (AV2013) were originally received from the China Veterinary Culture Collection Center and propagated in BHK-21 cells. The street virus GX/09, isolated from the brain of a dog that died of rabies in the Guangxi Province of China in 2009, was propagated in the brains of adult mice. All viruses were stored in a −70°C freezer before use for RNA extraction or challenge studies.

Construction of the LEP and HEP full-length cDNA clones. Viral RNA was extracted with an RNeasy minikit (Qiagen, Valencia, CA). The extracted RNA was subjected to reverse transcription-PCR (RT-PCR) using high-fidelity Pfx DNA polymerase (Invitrogen Corp., Carlsbad, CA) to generate three overlapping PCR fragments (F1, F2, and F3) of the entire viral genome (Fig. 1). The full-length viral genome RNA transcription plasmids were constructed as previously described by Inoue et al. (20). The assembled cDNA containing the sequence of the hammerhead ribozyme sequence (HamRz), the full-length (11,925-nucleotide) cDNA of the LEP or HEP strain genome in the antigenomic orientation, and the hepatitis delta virus ribozyme sequence (HdvRz) was inserted between the NheI and SmaI sites of the plasmid vector pCI. A PmeI restriction site was introduced as a genetic marker in the G-L noncoding region of the LEP and HEP cDNA by changing three nucleotides at position 4907 (T to G), 4910 (G to T), and 4912 (C to A) using a site-directed mutagenesis system (Invitrogen). The resulting full-length plasmids were designated pLEP and pHEP, respectively.

The open reading frames (ORFs) of the N, P, and L genes were PCR amplified from pLEP to construct helper plasmids. The amplified N, P, and L genes were each inserted between EcoRI and KpnI of the plasmid pCAGGS (37), and the resulting helper plasmids were designated pCA-NL, pCA-PL, and pCA-LL, respectively. The assembled full-length cDNA clones and the helper plasmids were confirmed by sequencing.

Construction of mutants and chimeric viral cDNA clones. The full-length cDNA clones of parental, mutated, and chimeric RVs are shown in Fig. 2. The mutant virus cDNA clone $pLEPG_{333Q}$, in which Arg at G333 of the LEP strain was mutated to Gln, and the $pHEPG_{333R}$ clone, in which Gln at G333 of HEP was mutated to Arg, were constructed by using a site-directed mutagenesis system (Invitrogen). The chimeric virus cDNA clone pLEP-G(H), in which the G gene ORF of LEP was replaced by that of HEP, was constructed in the following manner. One fragment containing the G gene of HEP was PCR amplified from pHEP, and another fragment containing the M gene of LEP was PCR amplified from pLEP. Both fragments were used as templates for an overlapping PCR. The PCR product was digested with XhoI and PmeI and then inserted into the same site of plasmid pLEP. The same method was used to construct the chimeric virus cDNA clone $pHEP\text{-}G(L)_{333Q}$, in which the G gene ORF of HEP was replaced by that of LEP with the G_{R333Q} mutation.

For construction of the chimeric virus cDNA clone $pLEPG_{333Q}$-L(H), in which the L gene ORF of $pLEPG_{333Q}$ was replaced by that of HEP, one fragment containing the L gene and the trailer sequence of HEP was amplified from pHEP, and another fragment containing part of the G gene, the φ gene, and part of the L gene of LEP was amplified from pLEP. Both fragments were then used as templates for an overlapping PCR. The PCR product was digested with PmeI and SmaI and then cloned into PmeI- and SmaI- predigested plasmid $pLEPG_{333Q}$. All of the sequences of the primers used in this study are available from the corresponding author upon request.

Virus rescue. BHK-21 cells were grown overnight to 80% confluence in 6-well plates in DMEM supplemented with 10% FBS. Cells were transfected with 4.0 μg of the full-length plasmid, 2 μg of pCA-NL, 1 μg of pCA-PL, and 1 μg of pCA-LL using Lipofectamine 2000 (Invitrogen) according to the manufacturer's protocol. After 4 to 6 h, the transfection medium was replaced with fresh DMEM supplemented with 10% FBS. After 3 days, supernatants were collected and transferred into wells containing BHK-21 cells and incubated another 3 days. Rescued viruses were examined by indirect fluorescence assay (IFA) with mouse serum against RV and fluorescein isothiocyanate (FITC)-conjugated goat-anti-mouse IgG. Supernatants from virus-positive culture wells were collected to propagate virus stock in BHK-21 cells. The sequences of recovered viruses were confirmed by sequencing of the entire viral genome.

Virus titration. Monolayers of NA or BHK-21 cells in 24-well plates were infected with 10-fold dilutions of virus suspension and incubated at 34°C. At 48 h postinfection, an IFA was performed. Foci were counted under a fluorescence microscope and calculated as focus-forming units/ml (FFU/ml). The *in vitro* neurotropism index was expressed as the logarithm of the titer of virus stock in NA cells subtracted by the logarithm of the titer of the same stock virus in BHK-21 cells.

Infection of mice. Virulence of the virus in adult mice was measured in 6-week-old female BALB/c mice (Vitalriver, Beijing). Groups of five mice were inoculated i.c. or intranasally (i.n.) with 30 μl of diluted virus or intramuscularly (i.m.) with 100 μl of diluted virus. After infection, mice were observed for clinical signs of disease, and body weight was recorded daily. The mouse 50% lethal dosage (MLD_{50}) of the viruses was calculated by the method of Reed and Muench (42).

Flow cytometric analysis of FITC annexin V staining. Apoptotic cells of the early stage were detected using a FITC annexin V apoptosis detection kit (BD Pharmingen, San Diego, CA). NA cells were infected with recombinant RVs at a multiplicity of infection (MOI) of 1 and incubated for 24 h at 34°C. Cells were washed twice with cold PBS and then resuspended in PBS and adjusted to a concentration of 1×10^6 cells/ml. Next, 10^5 cells were incubated with 5 μl of FITC annexin V and 5 μl propidium iodide (PI) for 15 min at 25°C in the dark. Afterward, 400 μl of binding buffer was added to each tube, and flow cytometry was performed on a BD FACSAria analyzer.

Western blotting. NA cells grown in 6-well plates were infected with different RV strains at an MOI of 1 and incubated for 24 h. G gene expression was confirmed by Western blotting. Briefly, cell extracts were analyzed by SDS-PAGE and then blotted to nitrocellulose membrane. The membrane was incubated with a mixture of mouse anti-G protein polyclonal antiserum, mouse anti-N protein polyclonal antiserum, and anti-β-actin monoclonal antibody (Santa Cruz Biotechnology). Bindings were visualized with 3,3′-

TABLE 1. Amino acid substitutions in N, P, M, G, and L proteins of the HEP strain compared to those of the LEP strain

Protein	Position	Substitution	
		LEP strain	HEP strain
N	13	Q	R
P	59	G	D
	84	D	N
	160	T	I
	277	I	L
	295	T	K
M	22	V	A
	97	I	V
G[a]	19	I	L
	40	E	G
	194	N	H
	204	G	D
	333	R	Q
	349	G	E
	425	E	K
	431	E	D
	436	N	K
	473	S	N
	476	E	G
L	75	V	G
	223	V	I
	431	L	R
	514	K	Q
	1226	P	S
	1567	R	Q
	1740	H	R
	1795	V	I

[a] The amino acid numbering in the G protein corresponds to the matured form that does not contain a signal peptide.

diaminobenzidine reagent after incubation with peroxidase-conjugated secondary antibodies.

Immunization and virus challenge. Four-week-old female BALB/c mice (groups of 10) were injected i.m. in the gastrocnemius muscle with 100 μl of serial 10-fold dilutions of rescued live RVs. After 3 weeks, mice were bled and injected i.m. with 100 μl of street virus GX/09 strain containing 50 MLD_{50}. Mice were observed for 4 weeks for clinical signs of rabies. Mice that showed definitive clinical signs of rabies, such as paralysis, tremors, and spasms, were euthanized by CO_2 intoxication. Survival rates obtained with the different vaccine dilutions for the different vaccination groups were compared.

Neutralizing antibodies assay. Mice were bled from the retro-orbital sinus under isoflurane inhalation anesthesia, and mouse sera were tested for virus-neutralizing antibodies (VNA) using the rapid fluorescent focus inhibition test (RFFIT), as described elsewhere (13, 47). Neutralization antibody titers, defined as the highest serum dilution that neutralizes 50% of the challenge virus, were normalized to international units (IU) using the World Health Organization anti-RV antibody standard. Geometric mean titers (GMT) were calculated from the titers of 10 mice of the same vaccination group.

Nucleotide sequence accession number. The sequence data for the Flury LEP and HEP strains in this study have been deposited in GenBank under accession numbers GU565703 and GU565704, respectively.

RESULTS

Genome comparison of Flury LEP and HEP strains. The LEP and HEP strains of Flury RV have similar genomic backgrounds but differ in their virulence levels in adult mice. Sequencing analyses revealed that the genomes of the LEP and HEP strains share 99.3% nucleotide sequence identity and a deduced amino acid homology of 99.8%, 98.3%, 99.0%, 97.8%, and 99.6% between the individual N, P, M, G, and L proteins, respectively. The two strains have identical intergenic regions between N/P, P/M, and M/G and one substitution in the G-L intergenic region. Sequences of the 3′ and 5′ terminal noncoding regions, which include the recognition and initiation site of the viral RNA polymerase, were completely conserved in the two viruses. The locations of amino acid substitutions in the N, P, M, G, and L proteins are indicated in Table 1. A total of 27 amino acid substitutions were found between these two strains.

Biological characterization of the wild type and the rescued strains. To investigate the molecular mechanism for virulence and attenuation of Flury RV, two infectious viruses, rLEP and rHEP, were rescued from the genomes of LEP and HEP, respectively. A PmeI restriction endonuclease site in the G-L noncoding region was generated as a genetic marker for both rescued viruses to distinguish them from wild-type LEP and HEP viruses. The growth of the rLEP and rHEP strains in cultured cells and their virulence in adult mice were determined and compared with those of their wild-type counterparts. The growth curves of the rLEP and rHEP strains were similar to the wild-type LEP and HEP strains, respectively, in both neuronal NA and nonneuronal BHK-21 cells (Fig. 3). The *in vitro* neurotropism index, defined as the infectivity ratio of a given virus in NA cells versus in BHK-21 cells, represents a key measurement of RV neuroinvasiveness and neurorvirulence (34). The rLEP and wild-type LEP strains appeared to be strongly neurotropic, having similar index values of 0.84 and

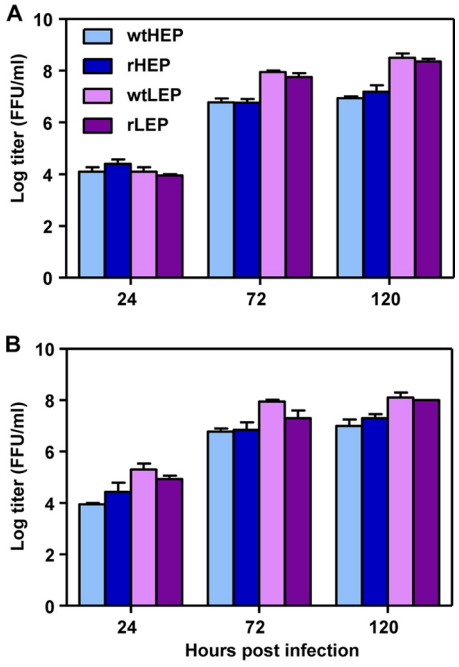

FIG. 3. Multistep growth curves of the rLEP, wtLEP, rHEP, and wtHEP viruses. NA (A) or BHK-21 (B) cells were infected with different viruses at an MOI of 0.01. The viral titers in infected cell supernatants were determined at different time points. Data shown are the mean titer ± standard deviations (SD).

TABLE 2. Growth titers of RV strains in NA and BHK cells

Strain	Titer (FFU/ml)[a]		Neurotropism index[b]
	NA	BHK-21	
wtLEP	3.7×10^8	5.3×10^7	0.84
rLEP	3.0×10^8	5.0×10^7	0.78
wtHEP	1.0×10^7	1.0×10^7	0
rHEP	2.0×10^7	2.0×10^7	0
$rHEPG_{333R}$	1.6×10^8	2.5×10^7	0.80
$rLEPG_{333Q}$	3.0×10^7	3.3×10^7	0
rLEP-G(H)	7.0×10^6	7.0×10^6	0
$rHEP\text{-}G(L)_{333Q}$	2.0×10^7	2.0×10^7	0
$rLEPG_{333Q}$-L(H)	1.0×10^7	1.0×10^7	0

[a] Virus titers were determined by using an IFA as described in Materials and Methods.

[b] The neurotropism index equals the logarithm of the titer in NA cells subtracted by the logarithm of the titer in BHK-21 cells.

0.78, respectively. As expected, both rHEP and wild-type HEP did not show any neurotropic characteristics (Table 2).

Virulence of rLEP, rHEP, and wild-type LEP and HEP in adult mice was determined by different inoculation routes, i.c., i.n., or i.m. The survival rates and disease progression of mice infected with different dosages of rLEP or wild-type LEP are shown in Fig. 4A to F. The rLEP strain killed adult mice by any inoculation route. The MLD_{50} and death time courses after i.c. or i.n. inoculation of rLEP were comparable to those of wild-type LEP (Fig. 4). Peripheral pathogenicity was assessed by i.m. inoculation. The MLD_{50} of rLEP by i.m. inoculation was 3.4×10^5 FFU, slightly higher than that of wild-type LEP. For wild-type LEP, only one of the five mice inoculated i.m. with 10^6 FFU wild-type LEP died, and the others exhibited hind leg paralysis. In contrast, all mice survived from i.c., i.n., or i.m. inoculation, even with 10^6 FFU of rHEP or wild-type HEP (Fig. 4G to L), without exhibiting any neurological signs, except that an about 3% body weight loss was observed in the first 3 days postinoculation with the i.c. group. These results suggested that the rescued viruses had biological properties and pathogenicities similar to those of their corresponding parental wild-type virus in the adult mouse.

Substitution of Arg with Gln at G333 eliminates LEP neuroinvasiveness but not its lethal phenotype in adult mice by i.c. inoculation. The Arg at position 333 of G is one of the most important determinants for neurotropism of RV. LEP has Arg at position 333 of G, while HEP has Gln at this position. We generated a HEP mutant virus, $rHEPG_{333R}$, in which the Gln at G333 was changed to Arg. As shown in Fig. 6, the multiple-step growth curve of the $rHEPG_{333R}$ strain in NA cells was similar to that of the rLEP strain. Meanwhile, the *in vitro* neurotropism index of $rHEPG_{333R}$ was significantly increased from 0 to 0.8, indicating that $rHEPG_{333R}$ had acquired the neurotropism property. Infection of adult mice confirmed that $rHEPG_{333R}$ was lethal (Fig. 4 M to O). The MLD_{50} by i.c., i.n., and i.m. inoculation routines were 0.3 FFU, 887 FFU, and 1.4×10^6 FFU, respectively. Theses results were consistent with other reports (49). The mutation at G333 is sufficient to cause HEP to become highly pathogenic in adult mice.

Based on these results, it was hypothesized that the mutation of LEP G333 from Arg to Gln should eliminate the neurotropism property and therefore attenuates the LEP virus in adult mice. To investigate this issue, an LEP mutant, $rLEPG_{333Q}$, in which the Arg at G333 was changed to Gln, was constructed. As shown in Table 2, $rLEPG_{333Q}$ lost its neurotropism property and had a neurotropism index value of 0 in cell culture. Infection by the i.m. route with the maximum dosage of 3×10^6 FFU did not kill adult mice (Fig. 4R), and all surviving mice did not show any signs of neurological disease. However, when inoculated by i.c. and i.n. routes, $rLEPG_{333Q}$ remained highly lethal in adult mice (Fig. 4P and Q). The MLD_{50}s by i.c. and i.n. routes were 36 FFU and 2.1×10^5 FFU, respectively. These results suggested that substitution of Arg with Gln at G333 eliminated only the peripheral neuroinvasiveness of LEP by i.m. inoculation but not its lethal phenotype in adult mice by i.c. or i.n. inoculation.

Gln mutation at G333 of $rLEPG_{333Q}$ reverted to Arg during replication in neurological tissues or cells. Infection by the i.m. route showed that $rLEPG_{333Q}$ had lost its neurotropism *in vitro* and its peripheral pathogenicity *in vivo*, but it was still able to kill adult mice by i.c. and i.n. infection. One possible explanation for these results is that the Gln mutation at G333 of $rLEPG_{333Q}$ may quickly revert back to Arg during replication and allow the virus to then spread among neurological cells. To confirm this hypothesis, total RNA extracted from the brain tissue of each mouse killed after inoculation with $rLEPG_{333Q}$ was used as a template to amplify the G gene by RT-PCR. The results revealed that Gln (CAA) at G333 of $rLEPG_{333Q}$ completely reverted to Arg (CGA) in all mice after one i.c. inoculation (Fig. 5C). Passage of the virus in NA cells showed that Gln (CAA) at G333 in $rLEPG_{333Q}$ was not stably maintained in NA cells *in vitro* and partially mutated back to Arg (CGA) within five passages (Fig. 5D). These results indicated that $rLEPG_{333Q}$ could not stably maintain the G_{R333Q} mutation in mouse brain tissue and NA cells. The virus reverted back to regain its neurotropism and highly pathogenic phenotype. In contrast, rHEP stably maintained Gln (CAG) at G333, in both *in vivo* infection in mice by i.c. inoculation (Fig. 5A) and *in vitro* passaging in NA cells for up to five passages (Fig. 5B).

The LEP genome backbone is responsible for the instability of Gln mutation at G333. To investigate if a specific property of the G gene itself or if the genome background of LEP is responsible for the reversion of the Gln mutation at G333 to Arg, we constructed two chimeric viruses. The $rHEP\text{-}G(L)_{333Q}$ virus was generated by replacing the ORF of the G gene of HEP with that of LEP in which the amino acid at G333 was mutated from Arg to Gln. This virus showed a growth pattern similar to that of rHEP in NA cells (Fig. 6). The neurotropism index of $rHEP\text{-}G(L)_{333Q}$ was 0 and was the same as that of rHEP (Table 2). The pathogenicity of $rHEP\text{-}G(L)_{333Q}$ was evaluated by i.c. inoculation in adult mice. All mice inoculated with 10^5 FFU of $rHEP\text{-}G(L)_{333Q}$ survived the infection and did not show any signs of neurological disease (Fig. 7). Another chimeric virus, rLEP-G(H), was generated by replacing the G gene ORF of LEP with that of HEP. The titers of rLEP-G(H) in NA cells were lower than that of rLEP and similar to those of rHEP (Fig. 6). The *in vitro* neurotropism index of rLEP-G(H) was 0 (Table 2). All mice inoculated with 10^5 FFU of rLEP-G(H) died within 12 days postinfection (Fig. 7). The viral genomic RNAs isolated from the brain of infected mice were extracted and sequenced. The results revealed that G333 of rLEP-G(H) had changed to Arg (CGG) from Gln (CAG) (Fig. 5E). In comparison, the Gln (CAA) at G333 of rHEP-

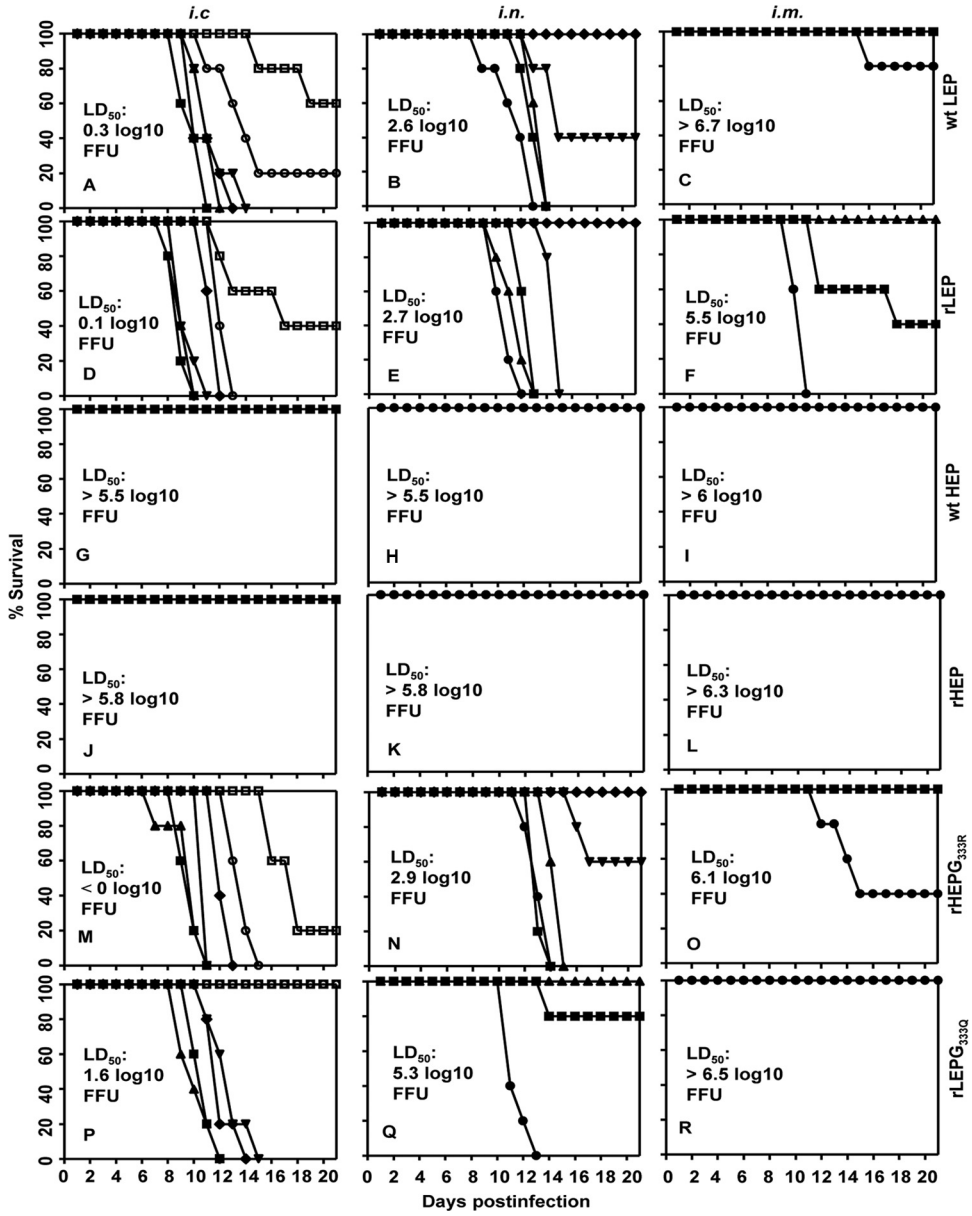

FIG. 4. Pathogenicity of different RVs in adult mice. Death patterns of mice i.c. infected with different dosages (10^0 to 10^6 FFU) of various viruses are shown. wtLEP (A), rLEP (D), wtHEP (G), rHEP (J), $rHEPG_{333R}$ (M), and $rLEPG_{333Q}$ (P), with different dosages from 10^0 to 10^5 FFU are shown. Death patterns of mice i.n. infected with wtLEP (B), rLEP (E), wtHEP (H), rHEP (K), $rHEPG_{333R}$ (N), and $rLEPG_{333Q}$ (Q), with different dosages of 10^2 to 10^6 FFU. Death patterns of mice i.m. infected with wtLEP (C), rLEP (F), wtHEP (I), rHEP (L), $rHEPG_{333R}$ (O), and $rLEPG_{333Q}$ (R), with different dosages from 10^4 to 10^6 FFU. The titers of the virus stocks used for inoculation were determined in BHK-21 cells (●, 10^6 FFU; ■, 10^5 FFU; ▲, 10^4 FFU; ▼, 10^3 FFU; ◆, 10^2 FFU; ○, 10^1 FFU; □,10^0 FFU.).

$G(L)_{333Q}$ was stably maintained after i.c. inoculation in mice (Fig. 5G).

rHEP-$G(L)_{333Q}$ and rLEP-G(H) was passaged an additional five times in NA cells at an MOI of 0.1. The viral genome RNAs were extracted from the fifth passage and subjected to RT-PCR and sequencing analysis. The results showed that the Gln (CAG) at G333 of rLEP-G(H) had partially changed to Arg (CGG) (Fig. 5F), whereas the Gln (CAA) at position G333 of rHEP-$G(L)_{333Q}$ remained stable after five passages in NA cells (Fig. 5H). These results strongly suggest that mutation from Gln to Arg at G333 does not happen randomly. Certain viral element(s) in the LEP genome backbone other than the G gene might be responsible for the instability of the Gln mutation at G333.

The L protein is related to the stability of Gln mutation at G333. The low fidelity of the RNA polymerase of negative-strand RNA viruses is the major reason for virus mutation. For this reason, we constructed another chimeric virus, $rLEPG_{333Q}$-L(H), in which the ORF of the L gene of $rLEPG_{333Q}$ was replaced with that of rHEP. Multistep growth kinetics analysis showed that $rLEPG_{333Q}$-L(H) replicated at a relatively lower rate, about 10-fold lower than

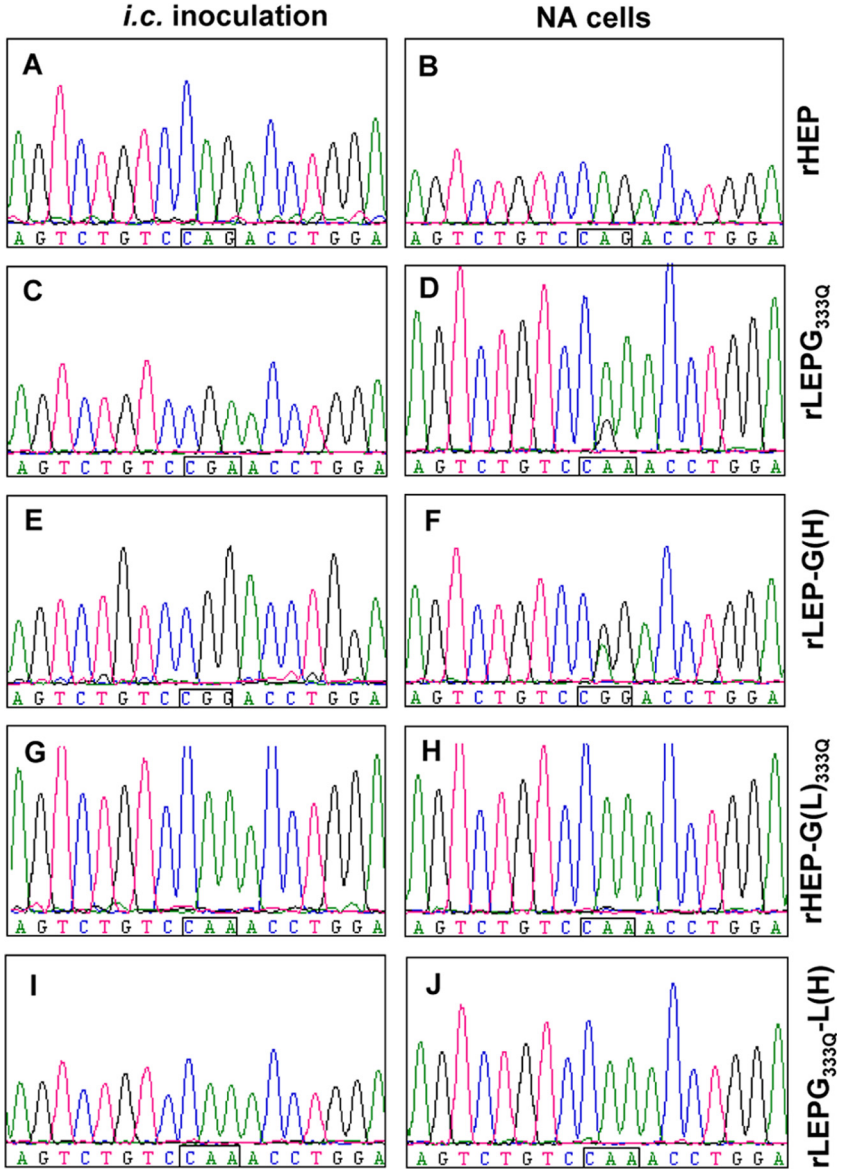

FIG. 5. Viral genome sequence analysis. The viral genome RNAs individually isolated from the brain tissues of mice i.c. inoculated with rHEP (A), rLEPG$_{333Q}$ (C), rLEP-G(H) (E), rHEP-G(L)$_{333Q}$ (G), and rLEPG$_{333Q}$-L(H) (I) were used as templates to perform RT-PCR and sequence analyses for the G gene. Viruses were also collected 2 days after infection with rHEP (B), rLEPG$_{333Q}$ (D), rLEP-G(H) (F), rHEP-G(L)$_{333Q}$ (H), and rLEPG$_{333Q}$-L(H) (J) viruses that had previously been passaged four times in NA cells. The viral genome RNAs were extracted at this later time point and used as templates to perform RT-PCR and sequence analyses for the G gene. The three nucleotides encoding the amino acid at G333 are boxed.

that of the rLEPG$_{333Q}$ (Fig. 6). All mice infected by the i.c. route with rLEPG$_{333Q}$-L(H) survived (Fig. 7) and showed no signs of neurological disease, except slight loss of body weight. This was similar to what was observed for rHEP-G(L)$_{333Q}$. The viral genome RNA from the brain of infected mice after inoculation with rLEPG$_{333Q}$-L(H) was subjected to RT-PCR and sequencing analysis. The results revealed that Gln (CAA) at G333 of rLEPG$_{333Q}$-L(H) remained unchanged (Fig. 5I). Further, rLEPG$_{333Q}$-L(H) also stably maintained Gln (CAA) at G333 after five passages in NA cells (Fig. 5J). These results indicated that the L protein is responsible for the stability of the Gln mutation at G333 of Flury RV.

The mutation of Arg to Gln at G333 is associated with a greater induction of early apoptosis by Flury RV. Several studies have shown that the attenuation of RV is associated with its ability to induce apoptosis in neuronal cells and that the G protein is responsible for triggering the apoptosis cascade (35, 39, 51). Annexin V binding, which detects the exposure of phosphatidylserine at the plasma membrane, is an early event in the apoptotic process (29). Therefore, we employed the annexin V binding assay to investigate if the attenuation of

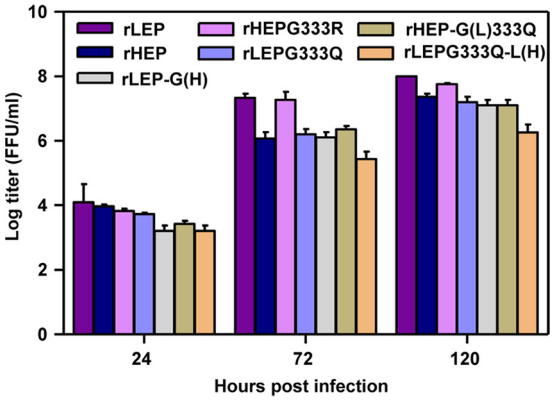

FIG. 6. Multistep growth curves of rLEP, rHEP, rHEPG$_{333R}$, rLEPG$_{333Q}$, rLEP-G(H), rHEP-G(L)$_{333Q}$, and rLEPG$_{333Q}$-L(H) in NA cells. NA cells were infected with different viruses at an MOI of 0.01. The virus titers in infected cell supernatants were determined at different time points. Data are presented as the means ± SD from three independent experiments.

Flury RV changed its ability to induce apoptosis in neuronal cells. The abilities of the different RVs to induce apoptosis in infected NA cells at 24 h postinfection were compared. The apoptotic cells were stained by the FITC-labeled annexin V, but were not stained by PI. The apoptotic cells infected by rLEP- or rHEPG$_{333R}$ were about 2.9 ± 0.7% or 2.8 ± 0.6%, respectively. These values were similar to that of uninfected cells (2.6 ± 0.6%). In contrast, rHEP, rLEPG$_{333Q}$, rHEP-G(L)$_{333Q}$, and rLEPG$_{333Q}$-L(H) induced significantly higher levels of apoptosis in NA cells, and the percentage of the apoptotic cells were 2.1, 2.4, 2.1, and 2.1 times higher, respectively, than that of the uninfected cells (Fig. 8A).

We compared the expression level of viral proteins in infected cells. NA cells infected with different recombinant viruses at an MOI of 1 were collected at 24 h postinfection and analyzed by Western blotting. The G protein and N protein were probed with a polyclonal serum against the G or N protein of LEP. The rLEP virus expressed amounts of G and N proteins similar to those of rLEPG$_{333Q}$, rHEP-G(L)$_{333Q}$, and rLEPG$_{333Q}$-L(H) in NA cells. Meanwhile, there was no significant difference in the expression level of G or N protein between NA cells infected by rHEP and rHEPG$_{333R}$ (Fig. 8B).

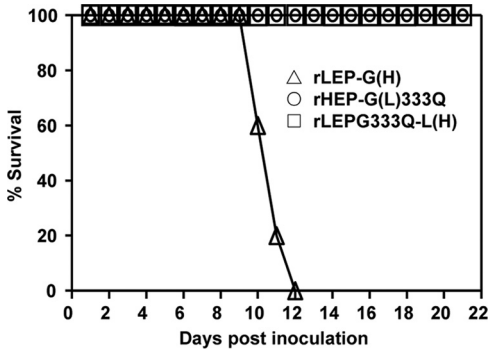

FIG. 7. Survival of adult mice infected i.c. with different RV mutants. Groups of 10 4-week-old BALB/c mice were i.c. inoculated with 10^5 FFU of the indicated virus and observed for 3 weeks.

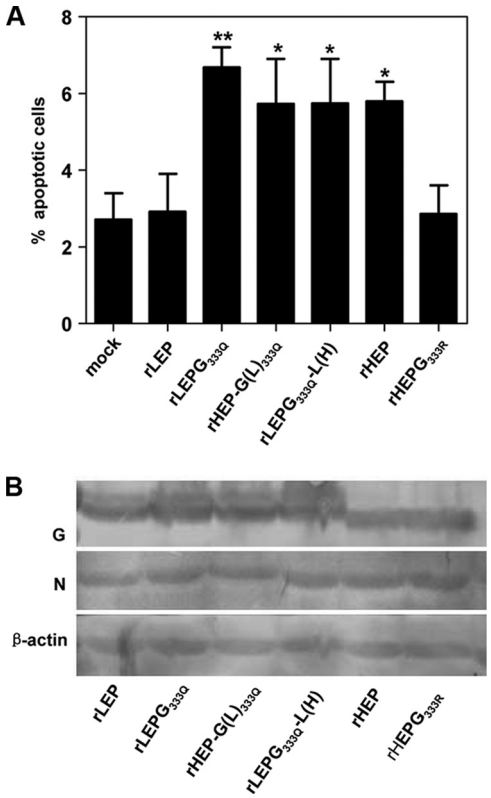

FIG. 8. Apoptotic cell detection and Western blotting of G protein expression. (A) NA cells were infected with rLEP, rHEP, rLEPG$_{333Q}$, rHEPG$_{333R}$, rHEP-G(L)$_{333Q}$, or rLEPG$_{333Q}$-L(H) at an MOI of 1. At 24 h postinfection, apoptotic cells were detected by using an FITC annexin V apoptosis detection kit, and flow cytometry was performed on a BD FACSAria analyzer. **, $P < 0.01$; *, $P < 0.05$. (B). NA cells were infected with rLEP, rHEP, rLEPG$_{333Q}$, rHEPG$_{333R}$, rHEP-G(L)$_{333Q}$, or rLEPG$_{333Q}$-L(H) at an MOI of 1. At 24 h postinfection, proteins were extracted from infected cells and were subjected to SDS-PAGE. Western blot analysis was conducted with a mixture of mouse anti-G polyclonal antiserum, anti-N polyclonal antiserum, and anti-β-actin monoclonal antibody. Bindings were visualized with 3,3′-diaminobenzidine reagent after incubation with peroxidase-conjugated secondary antibodies.

These results indicated that the higher levels of early apoptosis in NA cells induced by the recombinant viruses containing G$_{333Q}$ are not likely associated with an increase in the expression of G protein.

Attenuated recombinant viruses induced enhanced immune responses and more effective protection. It has been reported that attenuated RV is generally more effective at inducing protective immune responses. rLEPG$_{333Q}$-L(H) and rHEP-G(L)$_{333Q}$ have shown significant attenuation and genetic stability *in vivo* and *in vitro*. To test if these two recombinant viruses could serve as live vaccine candidates with improved safety and efficacy, we evaluated their immunogenicity in mice in comparison with rLEP and rHEP. Groups of 10 mice were i.m. immunized with 10^6 or 10^4 FFU of different RV strains and then subjected to lethal challenge with the rabies street virus GX/09. Immunization with 10^6 FFU of rLEPG$_{333Q}$-L(H) and rHEP-G(L)$_{333Q}$ induced similar levels of VNA, 3.6 IU and 3.3 IU, respectively, which were significantly higher than that induced by rHEP (1.6 IU [Fig. 9A]). In mice immunized with

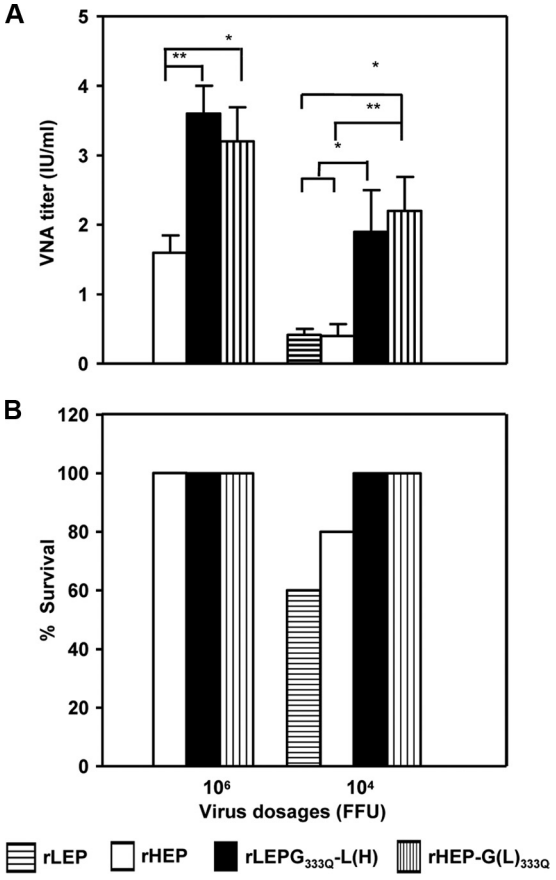

FIG. 9. Immunogenicity of rHEP-G(L)$_{333Q}$, rLEPG$_{333Q}$-L(H), rHEP, or rLEP after i.m. immunization of mice. Groups of 4-week-old mice were injected with 10^6 or 10^4 FFU of the different RVs. (A) Three weeks after inoculation, blood samples were obtained, and VNA titers were determined. Titers were normalized to IU by using the World Health Organization standard, and values are presented as the mean ± SD. (B) Three weeks after immunization, mice were infected i.m. with 50 MLD$_{50}$ of the street virus GX/09 and observed for 4 weeks. Percent survival was recorded. Statistically significant differences were determined by the *t* test (*, $P < 0.05$; **, $P < 0.01$.

the dosage of 10^4 FFU, average VNA titers induced by rLEPG$_{333Q}$-L(H) and rHEP-G(L)$_{333Q}$ were 1.9 IU and 2.2 IU, respectively, which were significantly higher than that of rLEP or rHEP (0.4 IU and 0.4 IU, respectively). These data were paralleled by the results of the challenge study. All mice vaccinated with the dosage of 10^6 FFU of three viruses, rLEPG$_{333Q}$-L(H), rHEP-G(L)$_{333Q}$, and rHEP, survived after being challenged with the GX/09 street virus at a dosage of 50 MLD$_{50}$. Immunization with 10^4 FFU of rLEPG$_{333Q}$-L(H) and rHEP-G(L)$_{333Q}$ also induced 100% protection against the challenge (Fig. 9B), while the mice vaccinated with 10^4 FFU of rLEP and rHEP were only partially protected, at 60% and 80%, respectively, from challenge with the GX/09 street virus (Fig. 9B), though the difference among these groups was not statistically significant. All 10 mice in the PBS-inoculated control group showed typical rabies disease signs and died within 12 days after challenge with the GX/09 street virus at a dosage of 50 MLD$_{50}$.

DISCUSSION

The molecular basis of rabies virus attenuation is not fully understood. To address this problem, we analyzed two genetically similar rabies viruses, the Flury LEP and Flury HEP strains. The LEP strain has an Arg at G333 and is lethal to adult mice by i.c. inoculation, whereas the HEP strain has a Gln at this position and is not lethal to adult mice by i.c. inoculation. The establishment of reverse genetics systems for the two strains has allowed us to delineate mechanisms that may be relevant to RV attenuation and pathogenicity in our study.

The mutant virus rHEPG$_{333R}$ regained lethality in adult mice by a single amino acid mutation at G333. These results are consistent with previous reports that Arg at G333 is a key determinant of virulence in most representative fixed viruses in adult mice (1, 5, 25, 36, 49, 53). The Arg at G333 may be indispensable for binding neuroreceptors, such as nicotinic acetylcholine receptor (27), neural cell adhesion molecule (NCAM) (52), and the low-affinity neurotrophin receptor p75NTR (54), though another study indicated that p75NTR is not essential for RV infection (55). Faber et al. reported that a lysine mutation from Asn at position 194 of G (G194) could functionally compensate for the mutation of G$_{R333Q}$ in the rabies vaccine strain SAD B19 and was associated with a reversion to the pathogenic phenotype (10). LEP has an Asn at G194, and HEP has a His at G194. Obviously, the His at G194 of HEP dose not functionally compensate for the G$_{R333Q}$ mutation in HEP. However, our results show that the single amino acid change at G333 is not enough to explain the virulence difference between LEP and HEP, as the mutant rLEPG$_{333Q}$ still showed a lethal phenotype in adult mice after i.c. or i.n. inoculation despite its loss of neurotropism *in vitro* and peripheral pathogenicity *in vivo*. Further analyses revealed that Gln at G333 of rLEPG$_{333Q}$ mutated back to Arg during *in vivo* and *in vitro* replication. The reversion occurred so quickly that the mouse host perhaps did not have enough time to develop sufficient adaptive immune responses against RV. Unlike the authors of a previous study with the RV SAD B19 strain (9), we did not observe significant dominance of a nonpathogenic glycoprotein gene over a pathogenic glycoprotein gene in recombinant rabies viruses during replication in mice brain tissues. In contrast, based on RT-PCR and sequencing analyses, our results showed that the virulent rLEPG$_{333R}$ from the reverted rLEPG$_{333Q}$ showed significant dominance over the attenuated rLEPG$_{333Q}$ during replication in mice brain tissue. Interestingly, significant replication dominance of virulent rLEPG$_{333R}$ was not observed during *in vitro* replication in NA cells.

The mutant rLEPG$_{333Q}$ has the same amino acid Gln at G333 as rHEP. However, these two viruses showed a significant difference in the genetic stabilities of the G$_{R333Q}$ mutations during replication in brain tissues or cells. RV G spikes function in low pH-induced fusion of the viral envelope with the host cell plasma and endosomal membranes in the early stage of the RV life cycle (19) and plays important roles in viral pathogenesis. We hypothesized that the G gene itself may be responsible for the genetic stability of the Gln mutation at G333. However, tests with the chimeric viruses rHEP-G(L)$_{333Q}$ and rLEP-G(H) clearly showed that a viral ele-

ment(s) in the genome backbone other than G may be responsible for the stability of the Gln mutation at G333. Additional tests with rLEPG$_{333Q}$-L(H) demonstrated that the L protein contributed to the stability of the G$_{R333Q}$ mutation of Flury RV.

The most concerning issue regarding the use of live attenuated RV vaccines is their high mutation rate. Several strains of attenuated RV consistently reverted rapidly to regain virulence after propagation in NA cells or suckling mouse brain, while others acquired increased virulence at a more gradual rate or not at all (3, 10). Many factors, including duration and route of infection, virus load, host immune response, and virus-host protein interaction may be involved (22). Despite these influences, the infidelity of the RNA polymerase of negative-strand RNA viruses could be the major factor responsible for the mutations introduced at a relatively high frequency. Recent evidence indicated that the RV polymerase complex also impacted virulence (58). The viral replication rate is controlled directly by the polymerase complex in tissue culture and has been shown to correlate inversely with the pathogenicity of RV (9, 35, 41). Analysis of the silver-haired bat-associated RV 18 (SHBRV-18) strain showed that the RV polymerase likely contributed to RV neuroinvasiveness (12). Similarly, specific mutations in influenza virus polymerase have also been shown to considerably increase the virus' activity in mammalian cells and to correlate with high virulence in mice (14–16, 18, 28, 48). However, there is still no direct evidence to explain how the polymerase affects the virulence of RV.

In our study, the L protein appeared to be closely associated with the attenuation of pathogenicity by stabilizing the Gln at G333, suggesting that the attenuation of Flury RV likely resulted from the harmonic coevolution of different elements in the viral genome. The critical importance of the L protein in transcription and replication is highlighted by its extreme sensitivity to mutation (4, 17). The amino acid sequence changes that we identified in the L protein of the HEP strain that differed from the LEP strain were V75G, V223I, L431R, K514Q, P1226S, R1567Q, H1740R, and I1795V. Phylogenetic analyses have subdivided the NNS L proteins into six conserved domains linked by variable regions (38). Of all these sequence differences in the HEP L protein, 1740R seems to be unique for the HEP strain. In contrast, all other RV strains with an Arg at G333, including LEP, SRV9 (AF499686), SAD-B19 (M31046), Ni-CE (AB128149), Nishigahara (AB044824), PV (NC_001542), rabies virus serotype 1 (AY956319), RC-HL (AB009663), SHBRV-18 (AY705373), and Mokola virus (Y09762), had H at position 1740 of the L protein. A statistical study showed that glycine as well as acidic (D and E) and basic (K, R, and H) amino acids are highly conserved and typically play a key role in L protein function and/or structure (26). Therefore, mutation at position 1740 is likely to be related to some functional change in the L protein that consequently influences the stability of the Gln mutation at G333. Further studies are needed to elucidate the significance of the amino acid substitutions.

Apoptosis is used by many neurotropic viruses as a mechanism of neuropathogenicity (32). The attenuation of RV is associated with its apoptotic ability in neuron cells (35). Several reports have suggested that the level of RV G expressed on the cell surface may be a critical factor in triggering apoptosis. Infection with recombinant RV expressing the proapoptotic protein cytochrome *c* induced a strong increase in apoptosis, antiviral immune response, and reduced pathogenicity (40). The contribution of apoptosis to immune responses may involve several mechanisms. The apoptotic cells can increase innate and adaptive immune responses and trigger the maturation and antigen presentation function of dendritic cells (43). Cells undergoing massive apoptosis could release factors to induce the activation of major histocompatibility complex (MHC) class I- and MHC class II-restricted T cells by mature dendritic cells (2, 44). Moreover, the apoptotic bodies have an exceptional ability to deliver antigens to professional antigen presenting cells (45). Our *in vitro* study with NA cells had shown that the lethal viruses, rLEP and rHEPG$_{333R}$, rarely induced apoptosis, while the highly attenuated viruses, rHEP, rLEPG$_{333Q}$, rHEP-G(L)$_{333Q}$, and rLEPG$_{333Q}$-L(H) induced significant apoptosis in NA cells. Our results are consistent with the observation that the pathogenicity of a particular RV strain correlates inversely with its ability to trigger apoptosis in neuronal cells (35). A previous study also observed that the induction of apoptosis is largely dependent on the expression levels of G protein (39), and overexpression of this protein results in enhanced apoptosis (11). Interestingly, our data showed that all four RV strains with the G$_{R333Q}$ mutation, rHEP, rLEPG$_{333Q}$, rHEP-G(L)$_{333Q}$, and rLEPG$_{333Q}$-L(H), induced significantly higher levels of apoptosis than the viruses with G$_{333R}$, rLEP and rHEPG$_{333R}$. However, there was no clear correlation between apoptosis induction and the viral replication titers or glycoprotein expression level among these viruses. Whether the differences in apoptotic induction observed with these viruses was caused by viral replication or changing the amino acid sequence of their glycoprotein still remains to be determined. It is possible that the Flury RV might use an additional direct mechanism to regulate apoptosis.

Due to its excellent immunogenicity, LEP has been widely used to generate inactivated RV vaccine for human and animals. In several countries, LEP also has been used as a live vaccine to control dog rabies, especially in countryside settings. However, the residual virulence of LEP obviously cannot meet the current international biosafety standards for a live vaccine. Previous reports demonstrated that enhanced apoptosis and attenuation of RV likely increases the induction of the antiviral immune response (11, 56). The chimeric virus rHEP-G(L)$_{333Q}$ or rLEPG$_{333Q}$-L(H) showed significant induction of apoptosis in NA cells and attenuation in mice. We therefore investigated whether these two viruses would be able to serve as modified live vaccine candidates. Immunization and challenge study results showed that rHEP-G(L)$_{333Q}$ or rLEPG$_{333Q}$-L(H) induced significantly higher VNA responses and more effective protection than rLEP and rHEP. Since rHEP-G(L)$_{333Q}$ and rHEP had similar replication titers in NA cells, we can infer that the G protein of LEP is more immunogenic than that of HEP.

In summary, we used the RV Flury virus strains LEP and HEP as models to investigate the attenuation mechanism of RV. Our results confirmed that the G$_{R333Q}$ mutation is crucial in the attenuation of Flury RV in mice. The G$_{R333Q}$ mutation was maintained only in the HEP genome background but not in the LEP genome background during replication in mouse

neural tissue or cell culture. Additionally, studies with chimeric viruses revealed that the L gene determines the genetic stability of the G_{R333Q} mutation during virus replication. The recombinant viruses containing the G gene with the G_{R333Q} mutation from LEP and the L gene of HEP showed significant improvement in genetic stability, attenuation, enhancement of apoptosis, and immunogenicity. These results strongly suggest that attenuation of Flury virus results from the harmonic coevolution of G and L elements. The findings of this study provide important information for the generation of safer and more effective modified live rabies vaccines.

ACKNOWLEDGMENTS

We thank Gloria Kelly for editing the manuscript.

This work was supported by grants from the Chinese National S&T Plan 2009ZX10004-214, by the Chinese National Key Basic Research Program (973) 2005CB523200, and by the Emory University GHI program.

REFERENCES

1. **Anilionis, A., W. H. Wunner, and P. J. Curtis.** 1981. Structure of the glycoprotein gene in rabies virus. Nature **294:**275–278.
2. **Chattergoon, M. A., J. J. Kim, J. S. Yang, T. M. Robinson, D. J. Lee, T. Dentchev, D. M. Wilson, V. Ayyavoo, and D. B. Weiner.** 2000. Targeted antigen delivery to antigen-presenting cells including dendritic cells by engineered Fas-mediated apoptosis. Nat. Biotechnol. **18:**974–979.
3. **Clark, H. F.** 1980. Rabies serogroup viruses in neuroblastoma cells: propagation, "autointerference," and apparently random back-mutation of attenuated viruses to the virulent state. Infect. Immun. **27:**1012–1022.
4. **Collins, P. L., L. E. Hightower, and L. A. Ball.** 1980. Transcriptional map for Newcastle disease virus. J. Virol. **35:**682–693.
5. **Conzelmann, K. K., J. H. Cox, L. G. Schneider, and H. J. Thiel.** 1990. Molecular cloning and complete nucleotide sequence of the attenuated rabies virus SAD B19. Virology **175:**485–499.
6. **Dietzschold, B., M. Schnell, and H. Koprowski.** 2005. Pathogenesis of rabies. Curr. Top. Microbiol. Immunol. **292:**45–56.
7. **Dietzschold, B., W. H. Wunner, T. J. Wiktor, A. D. Lopes, M. Lafon, C. L. Smith, and H. Koprowski.** 1983. Characterization of an antigenic determinant of the glycoprotein that correlates with pathogenicity of rabies virus. Proc. Natl. Acad. Sci. U. S. A. **80:**70–74.
8. **Etessami, R., K. K. Conzelmann, B. Fadai-Ghotbi, B. Natelson, H. Tsiang, and P. E. Ceccaldi.** 2000. Spread and pathogenic characteristics of a G-deficient rabies virus recombinant: an in vitro and in vivo study. J. Gen. Virol. **81:**2147–2153.
9. **Faber, M., M. L. Faber, J. Li, M. A. Preuss, M. J. Schnell, and B. Dietzschold.** 2007. Dominance of a nonpathogenic glycoprotein gene over a pathogenic glycoprotein gene in rabies virus. J. Virol. **81:**7041–7047.
10. **Faber, M., M. L. Faber, A. Papaneri, M. Bette, E. Weihe, B. Dietzschold, and M. J. Schnell.** 2005. A single amino acid change in rabies virus glycoprotein increases virus spread and enhances virus pathogenicity. J. Virol. **79:**14141–14148.
11. **Faber, M., R. Pulmanausahakul, S. S. Hodawadekar, S. Spitsin, J. P. McGettigan, M. J. Schnell, and B. Dietzschold.** 2002. Overexpression of the rabies virus glycoprotein results in enhancement of apoptosis and antiviral immune response. J. Virol. **76:**3374–3381.
12. **Faber, M., R. Pulmanausahakul, K. Nagao, M. Prosniak, A. B. Rice, H. Koprowski, M. J. Schnell, and B. Dietzschold.** 2004. Identification of viral genomic elements responsible for rabies virus neuroinvasiveness. Proc. Natl. Acad. Sci. U. S. A. **101:**16328–16332.
13. **Feyssaguet, M., L. Dacheux, L. Audry, A. Compoint, J. L. Morize, I. Blanchard, and H. Bourhy.** 2007. Multicenter comparative study of a new ELISA, PLATELIA RABIES II, for the detection and titration of anti-rabies glycoprotein antibodies and comparison with the rapid fluorescent focus inhibition test (RFFIT) on human samples from vaccinated and non-vaccinated people. Vaccine **25:**2244–2251.
14. **Gabriel, G., B. Dauber, T. Wolff, O. Planz, H. D. Klenk, and J. Stech.** 2005. The viral polymerase mediates adaptation of an avian influenza virus to a mammalian host. Proc. Natl. Acad. Sci. U. S. A. **102:**18590–18595.
15. **Gabriel, G., A. Herwig, and H. D. Klenk.** 2008. Interaction of polymerase subunit PB2 and NP with importin alpha1 is a determinant of host range of influenza A virus. PLoS Pathog. **4:**e11.
16. **Gabriel, G., K. Klingel, O. Planz, K. Bier, A. Herwig, M. Sauter, and H. D. Klenk.** 2009. Spread of infection and lymphocyte depletion in mice depends on polymerase of influenza virus. Am. J. Pathol. **175:**1178–1186.
17. **Galloway, S. E., and G. W. Wertz.** 2009. A temperature sensitive VSV identifies L protein residues that affect transcription but not replication. Virology **388:**286–293.
18. **Gao, Y., Y. Zhang, K. Shinya, G. Deng, Y. Jiang, Z. Li, Y. Guan, G. Tian, Y. Li, J. Shi, L. Liu, X. Zeng, Z. Bu, X. Xia, Y. Kawaoka, and H. Chen.** 2009. Identification of amino acids in HA and PB2 critical for the transmission of H5N1 avian influenza viruses in a mammalian host. PLoS Pathog. **5:**e1000709.
19. **Gaudin, Y., R. W. Ruigrok, M. Knossow, and A. Flamand.** 1993. Low-pH conformational changes of rabies virus glycoprotein and their role in membrane fusion. J. Virol. **67:**1365–1372.
20. **Inoue, K., Y. Shoji, I. Kurane, T. Iijima, T. Sakai, and K. Morimoto.** 2003. An improved method for recovering rabies virus from cloned cDNA. J. Virol. Methods **107:**229–236.
21. **Ito, N., M. Takayama, K. Yamada, M. Sugiyama, and N. Minamoto.** 2001. Rescue of rabies virus from cloned cDNA and identification of the pathogenicity-related gene: glycoprotein gene is associated with virulence for adult mice. J. Virol. **75:**9121–9128.
22. **Kissi, B., H. Badrane, L. Audry, A. Lavenu, N. Tordo, M. Brahimi, and H. Bourhy.** 1999. Dynamics of rabies virus quasispecies during serial passages in heterologous hosts. J. Gen. Virol. **80:**2041–2050.
23. **Koprowski, H., J. Black, and D. J. Nelsen.** 1954. Studies on chick-embryo-adapted-rabies virus. VI. Further changes in pathogenic properties following prolonged cultivation in the developing chick embryo. J. Immunol. **72:**94–106.
24. **Koprowski, H., and H. R. Cox.** 1948. Studies on chick embryo adapted rabies virus; culture characteristics and pathogenicity. J. Immunol. **60:**533–554.
25. **Lai, C. Y., and B. Dietzschold.** 1981. Amino acid composition and terminal sequence analysis of the rabies virus glycoprotein: identification of the reading frame on the cDNA sequence. Biochem. Biophys. Res. Commun. **103:**536–542.
26. **Le Mercier, P., Y. Jacob, and N. Tordo.** 1997. The complete Mokola virus genome sequence: structure of the RNA-dependent RNA polymerase. J. Gen. Virol. **78:**1571–1576.
27. **Lentz, T. L., T. G. Burrage, A. L. Smith, J. Crick, and G. H. Tignor.** 1982. Is the acetylcholine receptor a rabies virus receptor? Science **215:**182–184.
28. **Li, Z., H. Chen, P. Jiao, G. Deng, G. Tian, Y. Li, E. Hoffmann, R. G. Webster, Y. Matsuoka, and K. Yu.** 2005. Molecular basis of replication of duck H5N1 influenza viruses in a mammalian mouse model. J. Virol. **79:**12058–12064.
29. **Martin, S. J., C. P. Reutelingsperger, A. J. McGahon, J. A. Rader, R. C. van Schie, D. M. LaFace, and D. R. Green.** 1995. Early redistribution of plasma membrane phosphatidylserine is a general feature of apoptosis regardless of the initiating stimulus: inhibition by overexpression of Bcl-2 and Abl. J. Exp. Med. **182:**1545–1556.
30. **Mazarakis, N. D., M. Azzouz, J. B. Rohll, F. M. Ellard, F. J. Wilkes, A. L. Olsen, E. E. Carter, R. D. Barber, D. F. Baban, S. M. Kingsman, A. J. Kingsman, K. O'Malley, and K. A. Mitrophanous.** 2001. Rabies virus glycoprotein pseudotyping of lentiviral vectors enables retrograde axonal transport and access to the nervous system after peripheral delivery. Hum. Mol. Genet. **10:**2109–2121.
31. **Mebatsion, T., M. Konig, and K. K. Conzelmann.** 1996. Budding of rabies virus particles in the absence of the spike glycoprotein. Cell **84:**941–951.
32. **Mori, I., Y. Nishiyama, T. Yokochi, and Y. Kimura.** 2004. Virus-induced neuronal apoptosis as pathological and protective responses of the host. Rev. Med. Virol. **14:**209–216.
33. **Morimoto, K., H. D. Foley, J. P. McGettigan, M. J. Schnell, and B. Dietzschold.** 2000. Reinvestigation of the role of the rabies virus glycoprotein in viral pathogenesis using a reverse genetics approach. J. Neurovirol. **6:**373–381.
34. **Morimoto, K., D. C. Hooper, H. Carbaugh, Z. F. Fu, H. Koprowski, and B. Dietzschold.** 1998. Rabies virus quasispecies: implications for pathogenesis. Proc. Natl. Acad. Sci. U. S. A. **95:**3152–3156.
35. **Morimoto, K., D. C. Hooper, S. Spitsin, H. Koprowski, and B. Dietzschold.** 1999. Pathogenicity of different rabies virus variants inversely correlates with apoptosis and rabies virus glycoprotein expression in infected primary neuron cultures. J. Virol. **73:**510–518.
36. **Morimoto, K., A. Ohkubo, and A. Kawai.** 1989. Structure and transcription of the glycoprotein gene of attenuated HEP-Flury strain of rabies virus. Virology **173:**465–477.
37. **Niwa, H., K. Yamamura, and J. Miyazaki.** 1991. Efficient selection for high-expression transfectants with a novel eukaryotic vector. Gene **108:**193–199.
38. **Poch, O., B. M. Blumberg, L. Bougueleret, and N. Tordo.** 1990. Sequence comparison of five polymerases (L proteins) of unsegmented negative-strand RNA viruses: theoretical assignment of functional domains. J. Gen. Virol. **71:**1153–1162.
39. **Préhaud, C., S. Lay, B. Dietzschold, and M. Lafon.** 2003. Glycoprotein of nonpathogenic rabies viruses is a key determinant of human cell apoptosis. J. Virol. **77:**10537–10547.
40. **Pulmanausahakul, R., M. Faber, K. Morimoto, S. Spitsin, E. Weihe, D. C. Hooper, M. J. Schnell, and B. Dietzschold.** 2001. Overexpression of cytochrome *c* by a recombinant rabies virus attenuates pathogenicity and enhances antiviral immunity. J. Virol. **75:**10800–10807.

41. **Pulmanausahakul, R., J. Li, M. J. Schnell, and B. Dietzschold.** 2008. The glycoprotein and the matrix protein of rabies virus affect pathogenicity by regulating viral replication and facilitating cell-to-cell spread. J. Virol. **82:** 2330–2338.
42. **Reed, L., and Muench, H.** 1938. A simple method of estimating fifty percent endpoints. Am. J. Hyg. **27:**493–497.
43. **Restifo, N. P.** 2000. Building better vaccines: how apoptotic cell death can induce inflammation and activate innate and adaptive immunity. Curr. Opin. Immunol. **12:**597–603.
44. **Rovere, P., C. Vallinoto, A. Bondanza, M. C. Crosti, M. Rescigno, P. Ricciardi-Castagnoli, C. Rugarli, and A. A. Manfredi.** 1998. Bystander apoptosis triggers dendritic cell maturation and antigen-presenting function. J. Immunol. **161:**4467–4471.
45. **Sasaki, S., R. R. Amara, A. E. Oran, J. M. Smith, and H. L. Robinson.** 2001. Apoptosis-mediated enhancement of DNA-raised immune responses by mutant caspases. Nat. Biotechnol. **19:**543–547.
46. **Shimizu, K., N. Ito, T. Mita, K. Yamada, J. Hosokawa-Muto, M. Sugiyama, and N. Minamoto.** 2007. Involvement of nucleoprotein, phosphoprotein, and matrix protein genes of rabies virus in virulence for adult mice. Virus Res. **123:**154–160.
47. **Smith, J. S., P. A. Yager, and G. M. Baer.** 1973. A rapid reproducible test for determining rabies neutralizing antibody. Bull. World Health Organ. **48:**535–541.
48. **Steel, J., A. C. Lowen, S. Mubareka, and P. Palese.** 2009. Transmission of influenza virus in a mammalian host is increased by PB2 amino acids 627K or 627E/701N. PLoS Pathog. **5:**e1000252.
49. **Takayama-Ito, M., K. Inoue, Y. Shoji, S. Inoue, T. Iijima, T. Sakai, I. Kurane, and K. Morimoto.** 2006. A highly attenuated rabies virus HEP-Flury strain reverts to virulent by single amino acid substitution to arginine at position 333 in glycoprotein. Virus Res. **119:**208–215.
50. **Takayama-Ito, M., N. Ito, K. Yamada, M. Sugiyama, and N. Minamoto.** 2006. Multiple amino acids in the glycoprotein of rabies virus are responsible for pathogenicity in adult mice. Virus Res. **115:**169–175.
51. **Thoulouze, M. I., M. Lafage, J. A. Montano-Hirose, and M. Lafon.** 1997. Rabies virus infects mouse and human lymphocytes and induces apoptosis. J. Virol. **71:**7372–7380.
52. **Thoulouze, M. I., M. Lafage, M. Schachner, U. Hartmann, H. Cremer, and M. Lafon.** 1998. The neural cell adhesion molecule is a receptor for rabies virus. J. Virol. **72:**7181–7190.
53. **Tordo, N., O. Poch, A. Ermine, G. Keith, and F. Rougeon.** 1986. Walking along the rabies genome: is the large G-L intergenic region a remnant gene? Proc. Natl. Acad. Sci. U. S. A. **83:**3914–3918.
54. **Tuffereau, C., J. Benejean, D. Blondel, B. Kieffer, and A. Flamand.** 1998. Low-affinity nerve-growth factor receptor (P75NTR) can serve as a receptor for rabies virus. EMBO J. **17:**7250–7259.
55. **Tuffereau, C., K. Schmidt, C. Langevin, F. Lafay, G. Dechant, and M. Koltzenburg.** 2007. The rabies virus glycoprotein receptor p75NTR is not essential for rabies virus infection. J. Virol. **81:**13622–13630.
56. **Wang, Z. W., L. Sarmento, Y. Wang, X. Q. Li, V. Dhingra, T. Tseggai, B. Jiang, and Z. F. Fu.** 2005. Attenuated rabies virus activates, while pathogenic rabies virus evades, the host innate immune responses in the central nervous system. J. Virol. **79:**12554–12565.
57. **Wu, X., X. Gong, H. D. Foley, M. J. Schnell, and Z. F. Fu.** 2002. Both viral transcription and replication are reduced when the rabies virus nucleoprotein is not phosphorylated. J. Virol. **76:**4153–4161.
58. **Yamada, K., N. Ito, M. Takayama-Ito, M. Sugiyama, and N. Minamoto.** 2006. Multigenic relation to the attenuation of rabies virus. Microbiol. Immunol. **50:**25–32.
59. **Yan, X., M. Prosniak, M. T. Curtis, M. L. Weiss, M. Faber, B. Dietzschold, and Z. F. Fu.** 2001. Silver-haired bat rabies virus variant does not induce apoptosis in the brain of experimentally infected mice. J. Neurovirol. **7:**518–527.